0363-5465/87/1505-0455$02.00/0
THE AMERICAN JOURNAL OF SPORTS MEDICINE, Vol. 15, No. 5

Magnetic resonance imaging of knee hyaline cartilage and intraarticular pathology*

EDWARD WOJTYS,†‡ MD, MARK WILSON,† MD, KENNETH BUCKWALTER,§ MD, ETHAN BRAUNSTEIN,§ MD, AND WILLIAM MARTEL,§ MD

From the †Section of Orthopaedic Surgery and the §Department of Radiology, University Hospitals, University of Michigan, Ann Arbor, Michigan

ABSTRACT

Injuries to the hyaline cartilage of the knee joint are difficult to diagnose without invasive techniques. Even though these defects may be the most important prognostic factors in assessing knee joint injury, they are usually not diagnosed until arthrotomy or arthroscopy. Once injuries to hyaline cartilage are found and/or treated, no technique exists to follow these over time. Plain radiographs, arthrograms, and even computed tomography fail to detail most hyaline cartilage defects.

We used magnetic resonance imaging (MRI) to evaluate five fresh frozen cadaver limbs and 10 patients whose pathology was known from arthrotomy or arthroscopic examination. Using a 0.35 Tesla superconducting magnet and spin-echo imaging technique with a head coil, we found that intraarticular fluid or air helped to delineate hyaline cartilage pathology. The multiplane capability of MRI proved to be excellent in detailing small (3 mm or more) defects on the femoral condyles and patellar surface. Cruciate ligaments were best visualized on sagittal oblique projections while meniscal pathology was best seen on true sagittal and coronal projections.

MRI shows great promise in providing a noninvasive technique of evaluating hyaline cartilage defects, their response to treatment, and detailed anatomical information about cruciate ligaments and menisci.

The diagnosis and treatment of injuries about the knee joint has evolved tremendously in recent years. The need to accurately detail ligament laxity has been established and our abilities to address those problems have improved. The arthroscope has enhanced our understanding of meniscal function and improved our treatment of meniscal pathology. Despite these recent advances, our ability to diagnose and treat hyaline cartilage defects has not improved significantly. In the long term, this portion of the knee joint anatomy is most important for function. If laxity problems are solved and meniscal lesions treated in the face of hyaline cartilage damage, the end result may not be worthwhile. Part of the reason for this dilemma has been the clinician's poor understanding of hyaline cartilage physiology.

Hyaline cartilage is an extremely complex substance at both the microscopic and macroscopic level. The homogenous appearance of cartilage masks its unique structure which provides properties unequaled by any other material. It can be deformed, yet it regains its original shape while distributing loads to subchondral bone in a protective manner. It is unequaled as a low-friction gliding surface. It quite often outlasts years of wear without obvious ability to repair itself. The complex interaction of its cells and matrix in a surface usually less than 5 mm makes this function possible.

Chondrocytes compose approximately 5% of hyaline cartilage volume, while matrix accounts for 95%. Matrix is 60% to 80% tissue fluid and 20% to 40% structural macromolecules. Collagen, proteoglycan, and glycoprotein comprise the macromolecules. The complex milieu produced by these components in a hydrophilic atmosphere which changes with age controls the activity of the enclosed chondrocyte.[11] The matrix and cellular organization is not homogenous. It is organized into zones and regions. Morphologic and biochemical differences between zones exist depending on depth from the articular surface.[11] The most superficial of the four zones is specialized for gliding with a high collagen content and a low proteoglycan concentration. The second zone is the middle or transitional zone. This area contains larger collagen fibers and increased proteoglycan content. The third zone is the deep or radial zone which consists of the highest proteoglycan concentration and the lowest water

* Presented at the 12th Annual Meeting of the AOSSM, July 1986, Sun Valley, Idaho.
‡ Address correspondence and reprint requests to: Edward Wojtys, MD, Med Sport, 24 Frank Lloyd Wright Drive, P.O. Box 1023, Ann Arbor, MI 48106-1023.

concentration. The fourth zone is that of calcified cartilage which contains mineralized matrix.

The ability of this layered structure to respond to injury depends upon the depth of the insult. Since the only blood supply available to cartilage is through subchondral bone, injuries that do not penetrate bone are called superficial and must rely on the avascular response of local cells. Insults that penetrate bone produce a more typical response to injury. Without vascular ingrowth and the influx of fibroblasts, repair of superficial defects is left up to the local chondrocytes. Chondrocytes from immature cartilage are capable of increasing metabolic activity.[21,46–47] However, mature chondrocytes show little potential for replication[49] unless a chronic injury situation such as degenerative arthritis is induced.[30,31,54,68,78,79] Despite their lack of cellular division, adult cartilage cells can increase matrix production in response to various stimuli.[9,10,34,35,37,39,43,44,48,50–55,62,71–73,76] Various authors have documented the ineffectual response of hyaline cartilage to superficial lacerations.[1,2,5,6,13,14,20,22,24,26,28,45,48,49,61,64,75] Others have stated that superficial lacerations remain stable and only occasionally produce early degenerative arthritis.[56,81]

Deep penetrating injuries through the subchondral plate, on the other hand, stimulate a response similar to that of vascular tissue, including hematoma formation, influx of fibroblasts, and vascular ingrowth.[13,14,16,17,19,23,36,45,56–58,64] Those factors besides depth of injury penetration which are important to the ability of hyaline cartilage to repair, remain open to investigation. Convery et al.[19] investigated the importance of defect size on the distal femoral condyles of horses. Defects less than 3 mm in diameter showed complete repair in 3 months, while none of those larger than 9 mm in diameter showed complete repair. Baker et al.[3] found that electrical fields induced by electrodes next to subchondral bone accelerated hyaline cartilage healing. Mitchell and Shepard[58] investigated the effects of compression on the healing of intraarticular fracture in rabbits using AO fixation. Compression of fracture fragments consistently produced better repair of hyaline cartilage defects.

Salter et al.,[70] in a classic study, showed the advantages of continuous passive motion (CPM) over immobilization or intermittent motion in healing articular cartilage defects. They used defects 1 mm in diameter in adolescent and adult rabbits to evaluate two indices of repair: nature of the reparative tissue and degree of metachromasia. They concluded that CPM increased the rate and completeness of healing at 4 weeks. O'Driscoll and Salter[60] advanced the potential usage of CPM by applying it to intraarticular autografts in New Zealand rabbits. They recognized the limited cellular response of hyaline cartilage and used the cambium layer of periosteum as a source for undifferentiated mesenchymal cells. They concluded that periosteum has chondrogenic potential, especially when subjected to CPM.

The ability to improve the repair potential of articular cartilage defects was investigated by others including Pridie[63] and Insall et al.,[32] who clinically used multiple drill holes through subchondral bone to induce a healing response. Mitchell and Shepard[57,58] first investigated this approach using distal femurs of adult rabbits. They placed multiple 1 mm drill holes through subchondral bone and then injected ^{3}H-thymidine 24 hours prior to sacrificing the rabbits to trace cartilage activity. At 2 and 4 months postdrilling there were good plugs of cartilage present with variable distance spread and considerable metabolic activity. However, at 8 and 12 months the cartilaginous appearance was less obvious and the repair tissue had become more fibrous. The tangential collagen appearance was lost and the surface had become fibrillated. Furukawa et al.[25] arrived at the same conclusions with their radiochemical analysis. At 6 months postinjury there was more collagen and less hexosamine than control. They suggested that the fibrous texture was due to the loss of proteoglycan rather than a change in collagen.

Because of the inherent inability of animals or humans to repair injured hyaline cartilage adequately, whether the injury is deep or superficial, there is an obvious need to detect those defects. Once detected, whether treated operatively or conservatively, there is a need to follow the natural history of these injuries. Arthroscopy has allowed surgeons to view more defects and attempt various treatment options. Investigating the ability to detect these defects was our goal in evaluating the knee joint with MRI. We hoped that this procedure would eventually allow sequential evaluations of those defects. Arthrography has proven ineffective in detecting such lesions,[27,33,80] just as plain radiographs and computerized tomography.

MRI is a relatively new technique that depends upon the resonance of protons in a magnetic field after excitation by radiofrequency energy. It produges high resolution cross-sectional body images with greater soft tissue contrast than radiographs or computed tomography.

The production of cross-sectional images with MRI was first demonstrated by Lauterbur in 1973.[38] Various studies since that time have investigated normal and pathologic anatomy of different parts of the body.[7,15,18,29,59] Recent applications to the normal intraarticular and extraarticular structures about the knee joint are promising.[40,41,42,65–67,77,82] Sagittal views demonstrate femoral condylar cartilage as well as cruciate ligaments, patellar tendon, quadriceps tendon, and menisci. Axial sections are best for the patellofemoral joint, patellar bone, and trochlea. Coronal images provide additional detail of femoral hyaline cartilage and menisci.

The advantages of MRI include enhanced soft tissue contrast and direct multiplanar capability for three-dimensional imaging.[83] The ability to vary tissue contrast through alternations in imaging pulse sequences as well as the direct multiplanar image acquisition greatly facilitates the ability to image soft tissue structures. MRI is noninvasive, with no known adverse effects on human tissue.[12] Some information may also be obtained on the chemical composition of the tissue or fluid.[8,59,83] Current disadvantages include the long scanning times, the dependence on patient cooperation, and, to a lesser degree, spatial resolution. Present cost of an MRI examination is approximately $800. With advances being made in computer software, though, it is predicted that within 18 months that cost may be reduced to one-fourth that amount.

Even though knee hyaline cartilage has been seen in normal knees, no studies have investigated the effectiveness of MRI in identifying hyaline cartilage defects. Sabiston et al.[69] were able to reliably visualize early osteophytes and capsular thickening in experimental osteoarthritis, but cartilage erosions were not reliably seen. The purpose of this study was to evaluate MRI as a tool in the noninvasive study of hyaline cartilage defects.

MATERIALS AND METHODS

A total of five fresh frozen cadaver knees and 10 patients were evaluated with MRI. The five fresh frozen cadaver knees were first evaluated for range of motion, instability, and general appearance. None showed evidence of previous surgery or injury.

Medial arthrotomies were performed in the cadavers. Inspection of the knee joints was carried out and the results recorded, including hyaline cartilage thickness, meniscal integrity, cruciate or patellar abnormalities. Discrete chondral defects were made of varying depth, width, and location. The dimensions of the defects were measured with calipers marked in 1 mm increments.

A total of 24 chondral defects was made under direct surgical control via arthrotomies in the cadaver knees. The location, dimension in three planes, and angle in degrees from the longitudinal axis of the diaphysis were recorded. Defects ranged in width from 2 to 13 mm, depth from 1 to 8 mm, and calculated removed volume from 6.3 to 1,144.0 mm^3. Two patellar defects were excluded from the study due to incomplete scans which did not include transaxial images.

A total of 10 patients' knees was scanned with MRI. Patients were selected from an orthopaedic patient population; all underwent arthroscopy. Three patients were scanned postoperatively and seven preoperatively. Ages ranged from 15 to 58 years. Selection was biased toward those patients with ligament instability symptoms, therefore increasing the likelihood of traumatic chondral defects. One patient did not have an effusion and his knee was injected with 22 cc of Ringer's lactate prior to the scan.

Patients and cadaver limbs were scanned in an identical manner. Spin-echo magnetic resonance images were obtained on a 0.35 Tesla (T) superconducting system operating at 15 Mhz (Diasonics, Inc., San Francisco, CA). A 30 cm "head" coil was used in lieu of a surface coil as it allowed complete visualization of the knee without repositioning and produced clearer images than the surface coil. Only one knee was placed in the coil during the examination; if necessary, the other limb was secured to the outside of the coil and supported with a pillow. No special hardware or software modifications were made to the equipment.

For the description that follows, TR refers to the repetition time of the 90° radio frequency excitation pulse used to generate the magnetic resonance signal. The term TE refers to the echo time, which is twice the time between the 90° excitation pulse and the 180° echo rephasing pulse used in spin-echo imaging. Several parameters are responsible for the generation of the MR signal; two important parameters are the T1 and the T2 relaxation times. These are intrinsic properties of proton magnetization and directly affect image contrast. Pure T1 and T2 images cannot be generated directly with spin-echo pulse sequences. However, by varying the TR and TE times of the imaging pulse sequence, T1 and T2 weighted images can be acquired. At intermediate magnetic field strengths (e.g., 0.35 T), T1 weighted images are typically acquired with a TR of 0.5 second and a TE of 30 msec. Typical T2 weighted images are acquired with a TR of 2.0 seconds and a TE of 60 msec.

A transaxial localizer scan (TR 0.1 second, TE 30 msec) was performed initially. The knee was repositioned if needed; a subsequent software update allowed electronic offset of position without moving the patient. High resolution images were acquired on a 256 × 256 matrix with a 24 cm field of view (0.95 mm/pixel). T2 weighted images were obtained with a TR of 2.0 seconds and a TE of 80 msec. This pulse sequence provided excellent contrast between joint fluid and cartilage while maintaining a good signal to

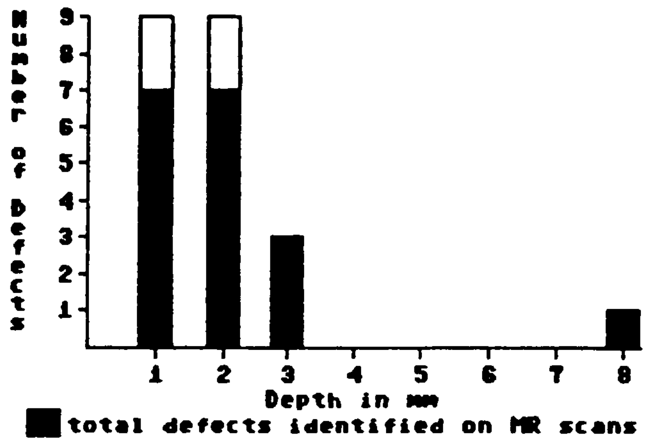

Figure 1. Depth versus defect detectability (cadaver group).

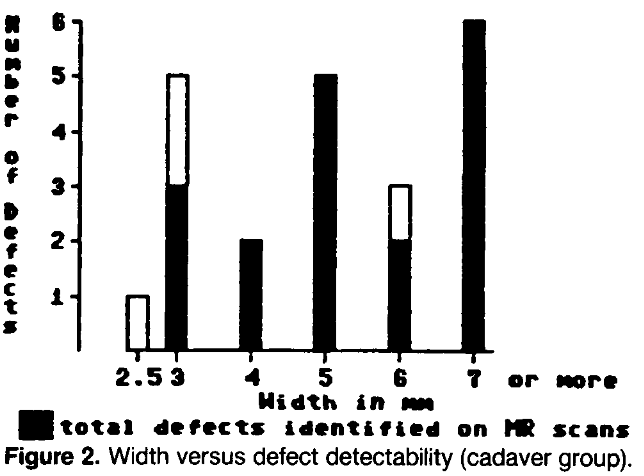

Figure 2. Width versus defect detectability (cadaver group).

noise ratio. A total of 16 5 mm thick contiguous images, covering 8 cm, were acquired simultaneously; this imaging sequence took approximately 17 minutes to perform. Direct coronal and sagittal images were obtained in all cases. Transaxial images were usually acquired, especially if patellar pathology was suspected; some of these were acquired with a TR of 1.5 seconds and a TE of 80 msec. The average examination took 90 minutes to perform.

Comparative evaluation of the blinded MRI reading and the known anatomical lesions was carried out. Some of the authors (radiologists) were not informed of the cadaver or patient findings until after the scans were read to prevent prejudice of interpretation. Findings from sagittal, coronal, axial, internally, and externally rotated sagittal images were tabulated. This study focused on the ability to visualize chondral defects and other hyaline cartilage pathology. Data included the size, location, and character of any hyaline cartilage pathology; however, findings relative to bone marrow, cruciate ligaments, menisci, synovium, capsule, and effusion were also noted. Comparison of the known pathology (from in vitro visualization or arthroscopic evaluation) was made with the MRI interpretations. The comparisons allow determination of false positive and false negative readings regarding identification of hyaline cartilage defects. Reliability of defect visualization was further broken down into subsets according to size, depth, volume, and location of the chondral defect. The tabulation of findings is separated into categories of hyaline cartilage defects (cadaver group, Figs. 1 and 2; patient group, Table 1), meniscal tears (Table 2), cruciate deficiencies (Table 3), and bone changes for both the cadavers and patients. The main focus of this study is chondral defects, although related or incidental findings are presented.

RESULTS

Hyaline cartilage defects

The normal appearance of hyaline cartilage is demonstrated in Figure 3. It is the grey region overlying the dark subchondral cortical bone. A total of 18 of 22 known hyaline cartilage defects in the cadaver knees were identified on the MRI scans (Table 1). The readers incorrectly interpreted one femoral condylar region as abnormal which did not have a visible defect at arthrotomy. The data is further broken down in Figures 1 and 2 by depth and width.

The data show that seven of nine of the 1 mm deep chondral defects were identified at scanning. Similarly, seven of nine of the 2 mm deep defects, all three of the 3 mm deep lesions, and the solitary 8 mm deep chondral fracture were seen. The widths were subgrouped as shown in Figure 2. Three of six of the lesions with a maximal width of 1 to 3 mm were identified. Likewise, 15 of the 16 chondral defects measuring greater than 3 mm in maximal width were seen.

TABLE 1
Patient hyaline cartilage defects (no. seen/no. present)

Depth of cartilage defect	Grade I	Grade II	Grade III
Patella	0/1	1/2	0/2
Tibia	0/1	0/0	1/2
Femur	1/3	7/8	4/4

TABLE 2
Meniscal tears

	No. lesions present	No. seen	False positive
Cadaver specimens	5	3	0
Subjects	2	2	4

TABLE 3
Anterior cruciate disruptions

	No. lesions present	No. seen	False positive
Cadaver	1	1	0
Patients	4	4	0

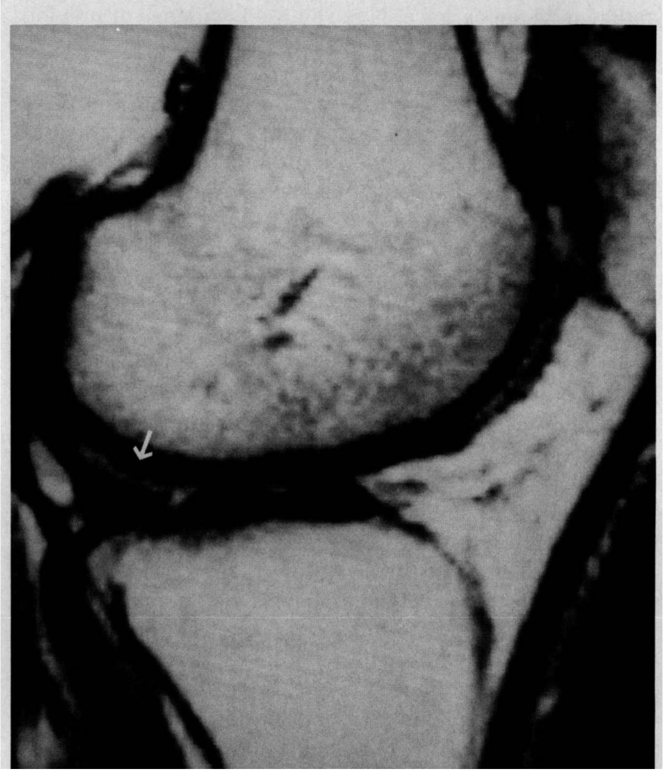

Figure 3. Sagittal view of knee demonstrates the dark cortical bone and overlying light hyaline cartilage.

The calculated volume of each defect missed at scanning measured 6.3, 9, 12, and 60 mm^3. The one defect of 60 mm^3 measured 5 by 6 by 2 mm deep. In retrospect, this defect was identifiable on the scan, but not obvious enough to call on the initial reading. It was located in the long axis of the femur, in the midportion of the condylar articular surface. With the knee in the extended position, the defect was obscured by the adjacent meniscus.

The 10 patients had a wide variety of hyaline cartilage

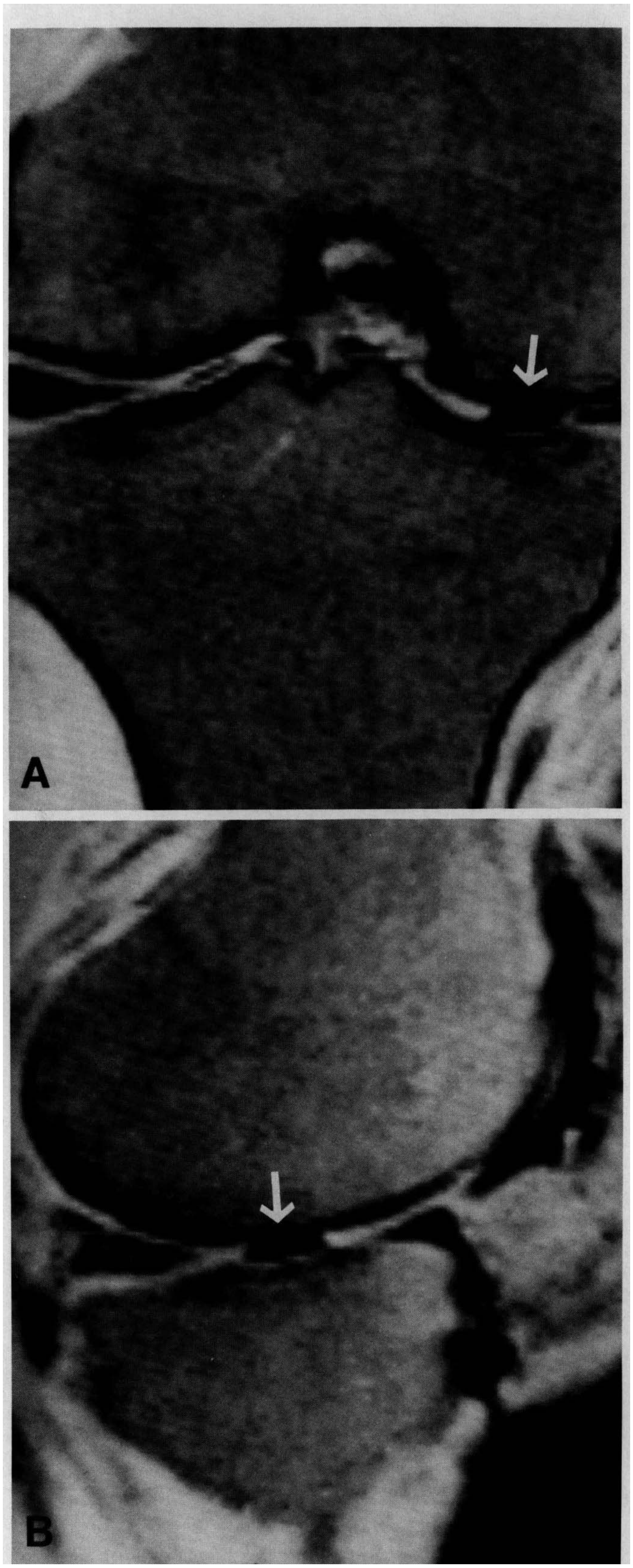

Figure 4. A, coronal view (magnified) demonstrates a 6 × 3 mm defect in hyaline cartilage on the lateral femoral condyle. The defect is outlined by air which is dark. B, sagittal view.

defects on the patella, femur, and tibia (Fig. 4). Arthroscopy identified a total of 21 hyaline cartilage lesions in eight patients; the other two patients had normal hyaline cartilage surfaces. These are broken down into groups by location and depth as depicted in Table 1. The grading system used refers to depth of the lesion, with Grade I referring to surface and texture changes but no cartilage substance loss; Grade II including partial thickness losses of hyaline cartilage but no exposed bone; and Grade III denoting exposed bone.

Only one of five Grade I lesions could be identified on MRI scans. Of these five, one was patellar, one was tibial, and three were femoral abnormalities.

There was a total of 10 Grade II lesions, 2 on the patella (Fig. 5) and 8 on the femoral surface. The MRI scan correctly identified eight of these ten defects ranging in size from 1.0 × 1.0 cm to 3.0 × 2.0 cm. The dimensions were estimated arthroscopically using a 3 mm probe tip as a reference guide. Of the two defects not seen on MRI, one was on the patella and the other on the femur.

The Grade III chondral fractures consisted of two on the tibial surface and four on the femur for a total of six. All but one of the defects were identified on MRI scan. Grade III defects ranged in size from 1.0 × 0.8 cm to 3.0 × 3.0 cm. The one defect not seen was a 0.8 × 1.0 cm lesion on the tibial surface, directly across from a kissing but slightly larger femoral defect.

The majority of chondral abnormalities, 15 of 21, were located on the femoral condylar surface, with no predilection for medial or lateral. Looking at just femoral Grade II and III lesions shows that 11 of the 12 defects ranging in size from 1.0 × 1.2 cm to 3.0 × 3.0 cm were correctly identified on MRI scan. The one lesion not seen was an irregular lateral femoral condyle lesion measuring 2.0 × 2.0 cm × 1.0 mm deep.

Figure 5. Transaxial view of the patellofemoral interface demonstrating 3 × 3 × 1 mm deep hyaline cartilage defect on the lateral patellar facet.

Meniscal lesions

Meniscal pathology was apparent in some of the cadaver specimens and the patients (Table 2). A total of five meniscal tears was created in the five cadaver knees; all were peripheral nondisplaced detachments greater than 2 cm in length. Of the five detachments, three were identified on the MRI scans with no false positive readings. The sagittal sections provided the best visualization of the peripheral meniscal detachments with coronal views adding more information. Fluid within the knee joint helped to identify the tear due to the high contrast between fluid and meniscal tissues.

The patient population had a total of four meniscal tears identified at arthroscopy. Of these four lesions, one was a peripheral displaced tear in a 9 year old with a discoid lateral meniscus (Fig. 6). Two patients were scanned postoperatively after partial meniscectomy had already been performed. The other meniscal injury was a posterior horn tear in the medial meniscus. This lesion and the discoid meniscus with detachment were correctly identified on MRI. Four

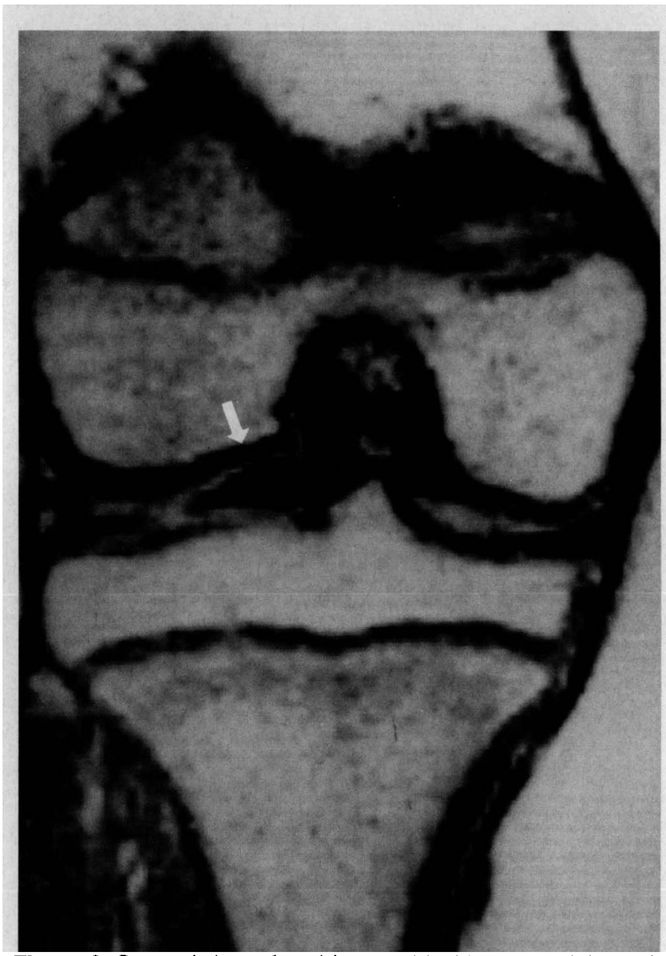

Figure 6. Coronal view of an 11 year old with open epiphyseal plates and a medially displaced torn discoid lateral meniscus. Note the adaptive molding of the medial half of this lateral femoral condyle and thinning of the hyaline cartilage between cortical bone and meniscus.

MRI scans were read as showing meniscal tears in patients without tears seen at arthroscopy.

Cruciate ligaments

In all 10 patients, the ACL was identified on MRI scan (Fig. 7A). There were four complete ACL tears of which all were correctly identified on MRI. On arthroscopic examination of the remaining six, four were felt to be normal and two were grossly intact but elongated, representing previous intrasubstance failure (Table 3). None of these six grossly intact ACLs were seen as abnormal on MRI. There were no false positive readings for cruciate pathology.

The posterior cruciate ligament (PCL) appeared redundant on the MRI in one patient. This was the only patient with a PCL deficiency on clinical examination demonstrated by posterior sag at the tibia at 90° of knee flexion and at arthroscopic evaluation.

Bone

Several miscellaneous changes in bone were seen on MRI. One patient with diffuse cartilage loss and synovitis had a large subchondral cyst. Two patients who had undergone arthroscopic drilling of Grade III femoral condyle lesions demonstrated changes in the subchondral bone and marrow elements immediately adjacent to these defects. The significance of these findings remains unclear. One patient without a cartilage defect showed changes in the marrow signal of one femoral condyle, but corresponding radiographs were normal. No bone scan was performed but osteonecrosis was suspected by history.

DISCUSSION

The importance of detecting hyaline cartilage defects is emphasized by its limited healing capacity. Our attempts to improve that healing capacity therapeutically would benefit immensely from a noninvasive method of determining the status of the cartilage and its response to treatment. MRI can provide visualization of hyaline cartilage. Eleven of 12 Grade II articular cartilage defects on the femoral condyle in our patient population were identified on MRI scans. The measurement of those defects are estimates made at arthroscopy by comparison to a 3 mm nerve hook tip. The precise sizing of the defects at arthroscopy is not as important as the fact that the overall reliability in identifying Grade II or deeper lesions was very good. The defects in the cadaver group were intentionally made smaller to test our ability to detect small defects. Fifteen of 16 defects that were 4 mm and larger in width along with those 3 mm and greater in depth were identified. Seven of 9 defects 1 mm in depth (Fig. 1) and 7 of 9 defects 2 mm in depth were correctly identified. These results suggest a consistent and sensitive method of detecting small cartilage defects. However, it should be kept in mind that the two groups of defects (cadavers and patients) were different in appearance and method of production. The defects in the patient group were

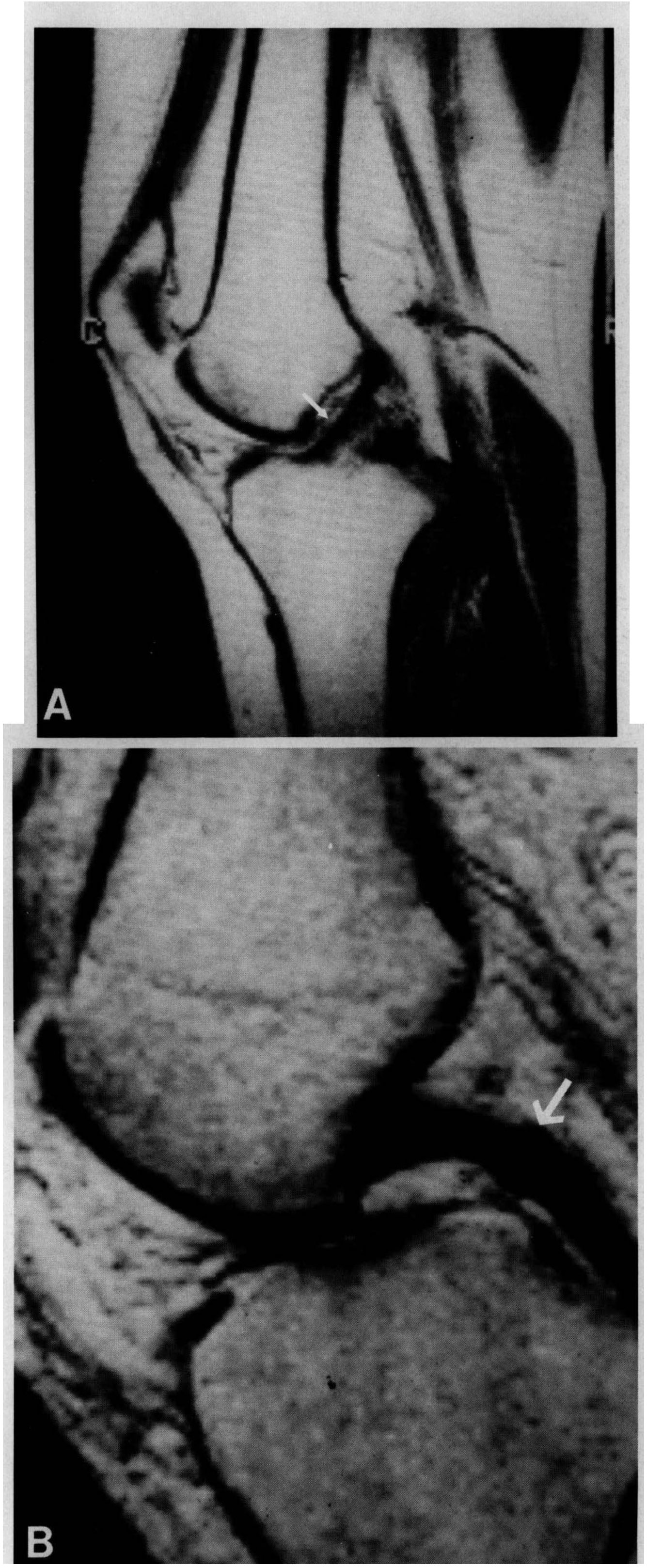

Figure 7. A, sagittal view of knee through the intracondylar notch demonstrates an intact ACL. B, sagittal view demonstrates PCL.

probably the result of compression or shearing forces. Those in the cadaver group were sharply dissected. We chose this technique instead of a more functional one in order to produce small defects with specific dimensions. In retrospect, the sharp borders produced by carving made the defects more identifiable.

Other factors should be kept in mind when evaluating the results of scanning small defects. First, in plane resolution was limited to 0.95 mm/pixel. Second, section thickness was 5 mm and partial volume averaging becomes a significant factor when the defects are narrower than the section width. Three of the four missed defects in the cadavers were less than 6 mm in width. Only one defect larger than 5 × 2 mm deep (5 mm) was missed.

We chose not to use the previously described MRI technique (Beltran et al.[4]) for knee imaging because the T2 weighted images on our scanner gave us the best tissue contrast, particularly in visualizing hyaline cartilage.

While it was not our intent to document meniscal, ligament, or bone defects, several findings were noted. Three of five peripheral meniscal detachments larger than 2 cm in the cadavers were detected. There was one false positive lateral meniscus tear in the patient group which, in retrospect, represented the popliteus hiatus. One peripherally detached and centrally torn discoid lateral meniscus was correctly identified. Our high number (four) of false positive scans suggesting meniscal tears is at least in part related to our scanning technique as well as the limited experience of the investigators.

The PCL was routinely visualized (Fig. 7B). The one torn PCL was correctly identified. The oblique sagittal images needed to optimally image the ACL (Fig. 7A) were not always obtained. Position changes such as hyperextension could have been used to help identify pathology in the cruciate ligaments. Since an intact appearance on a scan could not rule out an intrasubstance failure of the cruciate, this was not pursued.

Changes in the cancellous and cortical bone adjacent to several hyaline cartilage defects were seen in the patient population. Subchondral cysts were easily identified. Intensity differences in cancellous bone were sometimes noted adjacent to the hyaline cartilage defects. These increases in intensity on T2 weighted images are difficult to interpret since the scans were obtained after the defects were drilled at arthroscopy. This could represent edema related to the hyaline cartilage defect or possibly a reactive change in cancellous bone resulting from the drilling. We intend to continue monitoring these changes with serial scans.

In the future, we hope to improve the accuracy of MR imaging of the knee. Faster image acquisition, off-axis gradient selection, higher spatial resolution, different pulse sequences, better imaging coils, and additional experience will undoubtedly advance this goal. Because of the noninvasiveness and enhanced contrast with an effusion, MRI is ideally suited to the evaluation of acute trauma.

REFERENCES

1. Alfidi RJ, Haaga JR, El Yousef SJ, et al: Preliminary experimental results in humans and animals with a superconducting, whole-body, nuclear magnetic resonance scanner. *Radiology 143:* 175–181, 1982

2. Bailey RW, Habel DW: The fate of surgically created osteochondral fractures in adult and young dogs. *Surg Forum 11:* 438–440, 1960
3. Baker B, Becker RO, Spadaro J: A study of electrochemical enhancement of articular cartilage repair. *Clin Orthop 102:* 251–267, 1974
4. Beltran J, Noto AM, Mosure JC, et al: The knee: Surface-coil MR imaging at 1.5 T. *Radiology 159:* 747–751, 1986
5. Bennett GA, Bauer W: Further studies concerning the repair of articular cartilage and the reaction of normal joints of adult dogs to surgically created defects of articular cartilage, "Joint Mice" and patellar displacement. *Am J Pathol 8:* 499–524, 1932
6. Bennett GA, Bauer W: A study of the repair of articular cartilage in dog joints. *J Bone Joint Surg 17:* 141–150, 1935
7. Brady TJ, Rossen BR, Pykett IL, et al: NMR imaging of leg tumors. *Radiology 149:* 181–187, 1983
8. Brateman L: Chemical shift imaging: A review. *Am J Radiol 146:* 971–980, 1986
9. Brighton CT, Lane JM, Koh JK: In vitro rabbit articular cartilage organ model II. ^{35}S incorporation in various oxygen tensions. *Arthritis Rheum 17:* 245–252, 1974
10. Brighton CT, Shadle CA, Jiminez SA, et al: Articular cartilage preservation and storage. I. Application of tissue culture techniques to the storage of viable articular cartilage. *Arthritis Rheum 22:* 1093–1101, 1979
11. Buckwalter JA: AAOS Instructional Course, Lecture 313, 1986
12. Budinger TF: Nuclear magnetic resonance (NMR) in vivo studies: Known thresholds for health effects. *J Comput Assist Tomogr 5:* 800–811, 1981
13. Calandriccio RA, Gilmer WS, Jr: Proliferation, regeneration, and repair of articular cartilage of immature animals. *J Bone Joint Surg 44A:* 431–455, 1962
14. Campbell CJ: The healing of cartilage defects. *Clin Orthop 64:* 45–63, 1969
15. Chafetz NI, Genant HK, Moon KL, et al: Recognition of lumbar disk herniation with NMR. *Am J Radiol 141:* 1153–1156, 1983
16. Cheung HS, Cottrell WH, Stephenson K, et al: In vitro collagen biosynthesis in healing and normal rabbit articular cartilage. *J Bone Joint Surg 60A:* 1076–1081, 1978
17. Cheung HS, Lynch KL, Johnson RP, et al: In vitro synthesis of tissue specific Type II collagen by healing cartilage. I. Short-term repair of cartilage by mature rabbits. *Arthritis Rheum 23:* 211–219, 1980
18. Cohen MD, Klatte EC, Baehaer R, et al: Magnetic resonance imaging of bone marrow disease in children. *Radiology 151:* 715–718, 1984
19. Convery FR, Akeson WH, Keown GH: The repair of large osteochondral defects. An experimental study in horses. *Clin Orthop 82:* 253–262, 1972
20. DePalma AF, McKeever CD, Subin SK: Process of repair of articular cartilage demonstrated by histology and autoradiography with tritiated thymidine. *Clin Orthop 48:* 229–242, 1966
21. Elliott HC: Studies on articular cartilage. I. Growth mechanisms. *Am J Anat 58:* 127–145, 1936
22. Fischer AGT: Some researches into the physiological principles underlying the treatment of injuries and diseases of the articulations. *Lancet 2:* 451–548, 1923
23. Frost GE: Cartilage healing and regeneration. *J S Afr Vet Assoc 50:* 181–187, 1979
24. Fuller JA, Ghadially FN: Ultrastructural observations on surgically produced partial-thickness defects in articular cartilage. *Clin Orthop 86:* 193–205, 1972
25. Furukawa T, Eyre DR, Koide S, et al: Biochemical studies on repair cartilage resurfacing experimental defects in the rabbit knee. *J Bone Joint Surg 62A:* 79–89, 1980
26. Ghadially FN, Thomaw I, Oryschak AF, et al: Long term results of superficial defects in articular cartilage. A scanning electron microscope study. *J Pathol 121:* 213–217, 1977
27. Gilley JS, Gelman MI, Edson DM, et al: Chondral fractures of the knee. *Radiology 138:* 51–54, 1981
28. Haebler C: Experimentelle untersuchungen uber die regeneration des gelenkknorpels. *Bruns' Beitr Klin Chir 134:* 602–640, 1925
29. Worthington BS: Internal structural mapping by nuclear magnetic resonance. *Neurology 16:* 607–609, 1978
30. Hirotani H, Ito T: Chondrocyte mitosis in the articular cartilage of femoral heads with various diseases. *Acta Orthop Scand 46:* 979–986, 1975
31. Hulth A, Lindberg L, Telhag H: Mitosis in human osteoarthritic cartilage. *Clin Orthop 84:* 197–199, 1972
32. Insall J, Shoji H, Mauer V: High tibial osteotomy. *J Bone Joint Surg 55A:* 963–973, 1973
33. Ireland J, Trickey EL, Stoker OJ: Arthroscopy and arthrography of the knee: A critical review. *J Bone Joint Surg 62B:* 3–6, 1980
34. Kaye CF, Lippiello L, Mankin H, et al: Evidence for a pressure sensitive stimulus receptor system in articular cartilage. *Trans Orthop Res Soc 5:* 1, 1980
35. Kean DM, Worthington BS, Preston BJ, et al: NMR imaging of the knee: Example of normal anatomy and pathology. *Br J Radiol 56:* 355–364, 1983
36. Key JA: Experimental arthritis: The changes in joints produced by creating defects in the articular cartilage. *J Bone Joint Surg 13:* 725–739, 1931
37. Lane JM, Brighton CT, Menkowitz BJ: Anaerobic and aerobic metabolism in articular cartilage. *J Rheumatol 4:* 334–342, 1977
38. Lauterbur PC: Image formation by induced local interactions: Examples employing nuclear magnetic resonance. *Nature (Lond) 242:* 190–191, 1973
39. Lemperg RK, Bergenholtz A, Smith TWD: Calf articular cartialge in organ culture in a chemically defined medium. 2. Concentrations of glycosaminoglycans and (^{35}S)-Sulfate incorporation at different oxygen tensions. *In Vitro 11:* 291–301, 1975
40. Levinsohn EM, Baker BE: Prearthrotomy diagnostic evaluation of the knee: Review of 100 cases diagnosed by arthrography and arthroscopy. *AJR 134:* 107–111, 1980
41. Li DKB, Mayo J, Facke JS, et al: MRI of the knee with cruciate ligament injuries. Proceedings of the 70th Scientific Assembly and Annual Meeting of the Radiological Society of North America, Washington D.C., November 25–30, 1984
42. Li KC, Henkelman M, Poon PY, et al: MR imaging of the normal knee. *J Comput Assist Tomogr 8:* 1147–1154, 1984
43. Malemud CJ, Norby DP, Sokoloff L: Explant culture of human and rabbit articular chondrocytes. *Connect Tissue Res 6:* 171–179, 1978
44. Mankin HJ: Localization of tritiated thymidine in articular cartilage of rabbits. I. Growth in immature cartilage. *J Bone Joint Surg 44A:* 682–688, 1962
45. Mankin HJ: Localization of tritiated thymidine in articular cartilage of rabbits. II. Repair in immature cartilage. *J Bone Joint Surg 44A:* 688–698, 1962
46. Mankin HJ: The calcified zone (basal layer) of articular cartilage of rabbits. *Anat Rec 145:* 73–87, 1963
47. Mankin HJ: The effect of aging on articular cartilage. *Bull NY Acad Med 44:* 545–552, 1968
48. Mankin HJ: The reaction of articular cartilage to injury and osteoarthritis. Parts 1 and 2. *New Engl J Med 291:* 1285–1292, 1335–1340, 1974
49. Mankin HJ: The response of articular cartilage to mechanical injury. *J Bone Joint Surg 64A:* 460–466, 1982
50. Mankin HJ: The metabolism of articular cartilage in health and disease, in Burleigh PMC, Poole AR (eds): *Dynamics of Connective Tissue Macromolecules.* New York, American Elsevier, 1975, pp 327–353
51. Mankin HJ, Conger KA: The acute effects of intra-articular hydrocortisone on articular cartilage in rabbits. *J Bone Joint Surg 48A:* 1383–1388, 1966
52. Mankin HJ, Conger KA: The effect of cortisol on articular cartilage of rabbits. I. Effect of a single dose of cortisol on glycine C^{14} incorporation. *Lab Invest 15:* 794–800, 1966
53. Mankin HJ, Zarins A, Jaffe WL: The effect of systemic corticosteroids on rabbit articular cartilage. *Arthritis Rheum 15:* 593–599, 1972
54. Mankin HJ, Dorfman H, Lippiello L, et al: Biochemical and metabolic abnormalities in articular cartilage from osteo-arthritic human hips. II. Correlation of morphology with biochemical and metabolic data. *J Bone Joint Surg 53A:* 523–537, 1971
55. Mankin HJ, Trasher AZ, Weinberg EH, et al: Dissociation between the effect of bovine growth hormone in articular cartilage and in bone of the adult dog. *J Bone Joint Surg 60A:* 1071–1075, 1978
56. Meachim G, Roberts C: Repair of the joint surface from subarticular tissue in the rabbit knee. *J Anat 109:* 317–327, 1971
57. Mitchell N, Shepard N: The resurfacing of adult rabbit articular cartilage by multiple perforations through the subchondral bone. *J Bone Joint Surg 58A:* 230–233, 1976
58. Mitchell N, Shepard N: Healing of articular cartilage in intra-articular fractures in rabbits. *J Bone Joint Surg 62A:* 628–534, 1980
59. Moon KL Jr, Genant HK, Helms CA, et al: Musculoskeletal applications of nuclear magnetic resonance. *Radiology 147:* 161–171, 1983
60. O'Driscoll SW, Salter RB: The induction of neochondrogenesis in free intra-articular periosteal autografts under the influence of continuous passive motion. An experimental investigation in the rabbit. *J Bone Joint Surg 66A:* 1248–1257, 1984
61. Paget J: Healing of cartilage. *Clin Orthop 64:* 7–8, 1969
62. Phillips LS, Herington AC, Daughaday WH: Somatomedin stimulation of sulfate incorporation in porcine costal cartilage discs. *Endocrinology 94:* 856–863, 1974
63. Pridie KH: A method of resurfacing osteoarthritic knee joints, in Proceedings of the British Orthopaedic Association. *J Bone Joint Surg 41B:* 618–619, 1959
64. Puhl W, Dustmann HO, Quosdorf U: Tierexperimentell untersuchungen zur regeneration des gelenkknorpels. *Arch Orthop Unfallchir 74:* 352–365, 1973
65. Reicher MA, Rauschning W, Gold RH, et al: High resolution MRI of the knee joint: Normal anatomy. *AJR 145:* 895–902, 1985
66. Reicher MA, Bassett LW, Gold RH: High resolution MRI of the knee joint: Pathological correlations. *AJR 145:* 903–909, 1985
67. Reicher MA, Hartzman S, et al: Meniscal injuries: Detection using MR imaging. *Radiology 159:* 753–757, 1986

68. Rothwell AG, Bentley G: Chondrocyte multiplication in osteoarthritic articular cartilage. *J Bone Joint Surg 55B:* 588–594, 1973
69. Sabiston CP, Adams ME, Li DK: Assessment of experimental osteoarthritis by magnetic resonance imaging. Proceedings of the 32nd annual ORS, New Orleans, LA, Feb 17–20, 1986
70. Salter RB, Simmods DF, Malcolm BW, et al: The biological effect of continuous passive motion on the healing of full-thickness defects in articular cartilage. An experimental investigation in the rabbit. *J Bone Joint Surg 62A:* 1232–1251, 1980
71. Sandy JD, Brown HLF, Lowther DA: Control of proteoglycan synthesis. Studies on the activation of synthesis observed during culture of articular cartilages. *Biochem J 188:* 119–130, 1980
72. Schwartz ER, Adamy L: Effect of ascorbic acid on arylsulfatase activities and sulfated proteoglycan metabolism in chondrocyte cultures. *J Clin Invest 60:* 96–106, 1977
73. Schwartz ER, Kirkpatrick PR, Thompson RC: The effect of environmental pH on glycosaminoglycan metabolism by normal human chondrocytes. *J Lab Clin Med 87:* 198–205, 1976
74. Selesnick FH, Noble HB, Bachman DC, et al: Internal derangement of the knee: Diagnosis by arthrography, arthroscopy and arthrotomy. *Clin Orthop 198:* 26–30, 1985
75. Shands AR, Jr: The regeneration of hyaline cartilage in joints. An experimental study. *Arch Surg 22:* 137–178, 1931
76. Smith TWD, Duckworth T, Bergenholtz A, et al: Role of growth hormone in glycosaminoglycan synthesis by articular cartilage. *Nature (Lond) 253:* 269–271, 1975
77. Soundry M, Lanir A, Angel D, et al: Anatomy of the normal knee as seen by magnetic resonance imaging. *J Bone Joint Surg 68B:* 117–120, 1986
78. Telhag H: Mitosis of chondrocytes in experimental "osteoarthritis" in rabbits. *Clin Orthop 86:* 224–229, 1972
79. Telhag H: DNA synthesis in degenerated and normal joint cartilage in full-grown rabbits. *Acta Orthop Scand 44:* 604–610, 1973
80. Thijin CJP: Accuracy of double-contrast arthrography and arthroscopy of the knee joint. *Skeletal Radiol 8:* 187–192, 1982
81. Thompson RC Jr: An experimental study of surface injury to articular cartilage and enzyme responses within the joint. *Clin Orthop 107:* 239–248, 1975
82. Turner DA, Prodomos CC, Clark JW: MR imaging in detecting acute injury of ligaments of the knee. Proceedings of the 70th Scientific Assembly and Annual Meeting of the Radiological Society of North America, Washington D.C., November 25–30, 1984
83. Wolf GL, Popp C: NMR-A primer for medical imaging. SLACK Incorp, Thorofare, NJ, 1984

DISCUSSION

George Belhobek, MD, *Cleveland, Ohio:* The major focus of this paper is a discussion of the ability of MRI to visualize defects in the articular cartilage of the knee joint. MRI, by virtue of its ability to visualize articular cartilage with an MR signal intensity different from subchondral bone and its ability to image the joint in three separate planes, certainly has the potential to become a practical method of evaluating hyaline cartilage injuries.

I am impressed by the data collected by these investigators. They show MRI to have the ability to demonstrate cartilage defects with depth of 1 mm and with diameters of 1 to 3 mm. Most of the defects greater than 3 mm in diameter were seen. I must say I am surprised by the authors' ability to resolve such small lesions with their equipment and choice of pulse sequence. As stated in their paper, each MR slice thickness was 5 mm, which would mean that partial volume averaging would have to be a factor in demonstrating defects of less than 5 mm. Their use of a head coil rather than surface coils, and their use of T2 weighted images rather than T1 weighted images, which would also result in less than optimal image resolution.

One of the distinct disadvantages as stated by the authors is that MR imaging takes a long time to acquire diagnostic images, especially with T2 weighted sequences. Patient compliance for an examination that would take up to 90 minutes would be difficult, I believe. I am also interested to know whether the authors have a feeling for whether MRI has any potential in the early diagnosis of chondromalacia.

I would like to congratulate the authors on this thought-provoking and interesting paper. MRI certainly appears to have the potential to become a practical method of evaluating internal derangements of the knee in the future. Improvements in MRI technology to decrease scanning time and increase image resolution would certainly strengthen that potential.

Authors' Reply: The first issue addressed, the partial volume averaging concept, is a very valid point. In the cadavers there were very sharply defined hyaline cartilage defect edges, whereas in the patient group, there was a more ragged edge due to the method in which the defect was produced. I think that had some effect on our ability to detect the small defects in the cadavers. In the patient group the lack of a sharp edge made visualization of small defects more difficult.

Also, in patients, we use T2 weighted images. Effusion fluid within the knees produces a very bright signal collected in the defect, and that tends to be exaggerated at the T2 weighted images.

As far as early diagnosis and chondromalacia, our techniques involve detecting defects. Softening and fibrillation changes in early chondromalacia are probably not detectable at this point.